Geophysical Research Letters

RESEARCH LETTER
10.1029/2019GL085851

Key Points:
- Cloud microphysical property changes are found to correlate with marine biogenic aerosol concentrations
- A strong correlation is found between cloud droplet number concentrations and cloud condensation nuclei concentrations
- The width of the cloud droplet distribution is found to be more strongly correlated with cloud liquid water path than droplet concentration

Supporting Information:
- Supporting Information S1

Correspondence to:
K. Sinclair,
kenneth.sinclair@columbia.edu

Citation:
Sinclair, K., van Diedenhoven, B., Cairns, B., Alexandrov, M., Moore, R., Ziemba, L. D., & Crosbie, E. (2020). Observations of aerosol-cloud interactions during the North Atlantic aerosol and marine ecosystem study. *Geophysical Research Letters*, *47*, e2019GL085851. https://doi.org/10.1029/2019GL085851

Received 22 OCT 2019
Accepted 13 JAN 2020
Accepted article online 16 JAN 2020

Observations of Aerosol-Cloud Interactions During the North Atlantic Aerosol and Marine Ecosystem Study

Kenneth Sinclair[1,2], Bastiaan van Diedenhoven[1,3], Brian Cairns[1], Mikhail Alexandrov[1,3], Richard Moore[4], Luke D. Ziemba[4], and Ewan Crosbie[4]

[1]NASA Goddard Institute for Space Studies, New York, NY, USA, [2]Universities Space Research Association, Columbia, MD, USA, [3]Center for Climate Systems Research, Columbia University, New York, NY, USA, [4]NASA/Langley Research Center, Hampton, VA, USA

Abstract Clouds and their response to aerosols constitute the largest uncertainty in our understanding of 20th-century climate change. We present an investigation that determines linkages between remotely sensed marine cloud properties with in situ measurements of cloud condensation nuclei (CCN) and meteorological properties obtained during the North Atlantic Aerosols and Marine Ecosystems Study. The first two deployments of this campaign have geographically similar domains but occur in different seasons allowing the response of clouds to a range of CCN concentrations and meteorological conditions to be investigated. Well-defined connections between CCN and cloud microphysical properties consistent with the indirect effect are observed, as well as complex, nonlinear secondary effects that are partially supported by previously proposed mechanisms. Using the Research Scanning Polarimeter's remotely sensed effective variance parameter, correlation is found with liquid water path. In general, cloud macrophysical properties are found to better correlate with atmospheric state parameters than changes in CCN concentrations.

1. Introduction

Aerosol-cloud interactions refer to changes in cloud condensation nuclei (CCN) that modulate cloud microphysical and macrophysical properties. Many mechanisms of aerosol-cloud interactions have been identified (Fan et al., 2016; Lohmann & Feichter, 2005), including the "cloud albedo effect" or first indirect effect. This effect relates an increase in CCN to an increase in cloud droplet number concentration (N_d), which leads to changes in the radiative properties of the cloud (Twomey, 1977). For a fixed liquid water content, the increase in CCN also results in smaller cloud droplets.

While the effect of increased CCN on N_d and droplet size has been well established (King et al., 1993; Platnick et al., 2000 and Platnick & Twomey, 1994), effects on other cloud properties are more uncertain. For instance, the effect of increased CCN and N_d on the effective variance (v_{eff}) or width of a cloud droplet size distribution has yielded conflicting results with some studies finding that v_{eff} increases with N_d (Martin et al., 1994; Ackerman et al., 2000), while other studies have found the opposite relation (Liu & Daum, 2002; Lu & Seinfeld, 2006; Miles et al., 2000), which questions the existence of such relation. Furthermore, an increase in droplet number concentrations has been shown to increase or decrease cloud liquid water path (LWP) and cloud cover, depending on boundary layer humidity (Ackerman et al., 2004). Studies have found cases where increased N_d are also associated with an increase in cloud vertical extent (Christensen & Stephens, 2011), which may partially result from decreased entrainment (Ackerman et al., 2004; Bretherton et al., 2007). Conversely, other cases have been documented where increased entrainment leads to cloud thinning (Wood, 2007). Such secondary indirect effects can amplify or diminish the first indirect effect of aerosols on radiative fluxes. All secondary effects of CCN on cloud albedo are collectively termed the effective radiative forcing due to aerosol-cloud interactions (ERF_{aci}; Albrecht, 1989; Liou & Ou, 1989; Pincus & Baker, 1994).

Radiative forcing due to changes in cloud properties in the remote and unpolluted marine atmosphere is particularly sensitive to changes to CCN (Twomey, 1991; Wood, 2005). Several regional studies suggest that changes in marine CCN concentrations are related to variations in dimethlysulphide (DMS; Charlson et al., 1987; Andreae et al., 1995; Hegg et al., 1991; Sanchez et al., 2018). These variations in marine

boundary layer DMS have long been linked to a seasonal cycle in phytoplankton activity, which is highly variable in time and location (Bates et al., 1998; Quinn et al., 2000). The North Atlantic annual phytoplankton cycle correlates with insolation and is initiated by deep water mixing explained through the "dilution-recoupling hypothesis" (Boss & Behrenfeld, 2010). Previous studies have found various linkages between marine aerosols and cloud properties (e.g., Gultepe et al., 1996; O'Dowd et al., 1999; Raga & Jonas, 1993; Twohy et al., 2005). However, due to the complexity of interactions involved, the magnitude and sign of these feedbacks remain uncertain.

We present an investigation that determines linkages between remotely sensed marine cloud properties with in situ measurements of CCN and meteorological properties obtained during the North Atlantic Aerosols and Marine Ecosystems Study (NAAMES; Behrenfeld et al., 2019). Cloud properties are retrieved from measurements by the airborne Research Scanning Polarimeter (RSP). Within the investigation, emphasis is placed on covariation between our remotely sensed ν_{eff} parameter with CCN, N_d, and LWP because of RSP's unique ability to remotely sense the effective variance and the uncertainty associated with its covariability from prior studies (Miles et al., 2000). We assess the extent that marine aerosols impact cloud properties to determine which existing concepts are supported by our observational study. Meteorological effects are investigated in an attempt isolate the primary drivers of cloud properties. We integrate our findings and discuss plausible secondary linkages between aerosol, cloud, and meteorological properties within the context of existing concepts.

2. Data

NAAMES is a multiyear NASA-led ship and aircraft campaign that took place in the North Atlantic Ocean, roughly east of Newfoundland, Canada. One of the primary objectives of the campaign is to study annual variations of phytoplankton biomass and to determine how marine aerosols and clouds are influenced by plankton ecosystems in the North Atlantic. The remote marine location offers an excellent region to explore cloud property changes in a relatively nonpolluted environment (Behrenfeld et al., 2019). The first two deployments, which correspond to the minima and maxima in the phytoplankton lifecycle, provide the largest contrast in ocean and atmosphere conditions. NAAMES-1, occurring near the phytoplankton bloom minima, is characteristic of clean marine conditions, often influenced by cold air outbreak conditions. NAAMES-2, which took place near the phytoplankton bloom maxima, has higher CCN concentrations and is characteristic of a nonpolluted marine atmosphere. This investigation uses NAAMES-1 science flight data from 11/12/2015–11/23/2015 as well as NAAMES-2 science flight data from 5/18/2016–6/1/2016. During both campaigns, the NASA C-130 aircraft flew in situ and remote sensing legs in sequence, with the remote sensing legs flown at a nominal altitude of 6,500 m. This study focuses on measurements made during cloud modules, which are periods where the C-130 samples an area multiple times and at different altitudes, often including a flight leg above cloud top for remote sensing measurements, at cloud altitude to make in situ measurements as well as beneath cloud base to measure ocean surface and boundary layer properties (i.e., Behrenfeld et al., 2019). Spatially, the sampled areas are typically smaller than 200 by 200 km and are sampled for approximately 1.5–2.5 hr. Supporting information Figures S1–S12 show Moderate Resolution Imaging Spectroradiometer (MODIS) Aqua imagery for each science flight with overlain C-130 flight paths. It is important to note that using a single aircraft to sample cloud, aerosol, and meteorological properties introduces temporal and spatial uncertainty in the comparisons. The mean difference between remotely sensed observations and in situ measurements is approximately 30 min across all days.

The C-130 was outfitted with a suite of remote sensing and in situ instruments allowing characterization of the ocean, aerosols, clouds, and meteorological properties. Cloud properties of interest include N_d, effective radius (r_{eff}), ν_{eff}, cloud optical thickness (τ), LWP, cloud physical thickness (H), and cloud top height (CTH), which are retrieved from measurements by the airborne RSP. Aerosol concentrations and chemical composition are measured using in situ aerosol instruments. Wind speeds and relative humidity (RH) measurements are also made using in situ probes. The broad range of instruments aboard the C-130 provides an excellent opportunity to study aerosol, cloud, and meteorological interactions.

The RSP (Cairns et al., 1999) makes polarimetric and total intensity measurements in nine spectral bands in the visible/near infrared and shortwave infrared. The RSP is an along-track scanning instrument that makes 152 measurements at viewing angles spaced 0.8°, effectively sweeping about ±60° from nadir along the

aircraft's track. Multiple views of the same location allow the RSP to observe the sharply defined cloud bow feature originating from single-scattered light near cloud top. This allows microphysical properties to be retrieved from a mean penetration depth of 0.5 τ from cloud top (Miller et al., 2018). The cloud droplet size distribution is retrieved from information in the relative *shape* of the cloudbow structure (Alexandrov, Cairns, Emde, et al., 2012). Here the size distribution is assumed to be represented by a modified gamma function of which the effective radius, r_{eff}, and v_{eff} are retrieved. Since the retrieval is not based on the absolute intensity of the cloudbow feature, it is less affected by three-dimensional cloud structure, broken clouds, multilayered effects, and above-plane cirrus and aerosol layers than techniques based on shortwave reflectance measurements (Miller et al., 2018; Nakajima & King, 1990). Simulations show the polarimetric technique has a mean uncertainty of 0.1 μm in r_{eff} and approximately 10% in v_{eff} (Alexandrov, Cairns, Emde, et al., 2012). Furthermore, comparisons with in situ measurements at cloud top have shown agreement better than 1 μm for r_{eff} and in most cases better than 0.02 for v_{eff} (Alexandrov et al., 2018). The retrieved size distribution allows the extinction cross-section to be derived, which along with the CTH (Sinclair et al., 2017), τ, and the cloud physical thickness, H, allows N_d to be retrieved (Sinclair et al., 2019). The technique assumes a linearly increasing liquid water profile and N_d being constant through the depth of the cloud. Uncertainty in the conventional N_d retrieval approach is dominated by uncertainty in the r_{eff} retrieval, which scales to the power of 5/2 (e.g., Grosvenor et al., 2018), whereas the uncertainty in our polarimetric approach scales linearly with uncertainties in r_{eff} and τ. Cloud data are retrieved during five science flights during NAAMES-1, namely, 11/12/2015, 11/14/2015, 11/17/2015, 11/18/2015, and 11/23/2015 and six science flights during NAAMES-2, namely, 5/18/2016, 5/19/2016, 5/27/2016, 5/28/2016, 5/29/2016, and 5/30/2016. Science flights on 5/20/2016 and 6/1/2016 are omitted because of the lack of cloud retrievals, while 5/26/2016 is not included because this day is largely characterized by multilayered cloud systems as identified by the MODIS multilayer flag, which adversely impacts the RSP N_d retrieval.

While the RSP is able to provide accurate cloud property retrievals, in situ measurements are required to accurately characterize colocated aerosol concentrations and meteorological conditions. CCN measurements were made using the Droplet Measurement Technologies Streamwise Thermal Gradient Cloud Condensation Nuclei Counter (CCNC, Roberts & Nenes, 2005; Rose et al., 2008), which measures the CCN concentration over the water supersaturation range of 0.2–0.6%, binned in 0.05% increments, using Scanning Flow CCN Analysis (Moore & Nenes, 2009). In this analysis, we use CCN measured at 0.35% supersaturation because it allows smaller organic particles to sufficiently hydrate. Aerosol mass composition measurements are made by the aerosol mass spectrometer (AMS, Canagaratna et al., 2007), which measures accumulation mode aerosol sizes, has a lower bound detection limit of 0.002 $\mu g \cdot m^{-3}$ and was operating with a 10-s measurement interval. CCN and AMS measurements are used from all the same days on which cloud measurements are made. CCN and AMS observations are averaged throughout the cloud modules when the C-130 is out of cloud and between 100 and 2,000 m, which is assumed to be representative of the boundary layer.

Three-dimensional wind measurements are made using in situ wind probes on the C-130 and averaged to 5 Hz. Ambient RH measurements are made using a LICOR-7200 instrument. RH measurements are used when the C-130 is out of cloud and separated into two atmospheric layers, namely, a lower layer between 100 and 1,400 m and an upper layer ranging from 1,400 to 3,000 m. RH measurements are used from all days included in our analysis with the exceptions of 5/18/2016, 5/19/2016, and 5/27/2016 when the probes made few valid measurements. Lastly, precipitation measurements are made continuously from the R.V. Atlantis, which operated in the general area considered here, using a Vaisala WX520 Precipitation Sensor that measures precipitation using a piezoelectric sensor operating at 1 Hz and returning the rain rate quantity in millimeters per hour.

3. Results

Despite having similar geographic domains, averages of cloud, aerosol, and meteorological properties observed during NAAMES-1 and NAAMES-2 are distinct and summarized in Table S1. Generally, we find that between NAAMES-1 and NAAMES-2 cloud microphysical properties are taken from statistically different populations, while mean meteorological properties are not statistically different. CCN is measured at 0.35% supersaturation and the geometric mean is shown for CCN as well as N_d. Arithmetic mean values

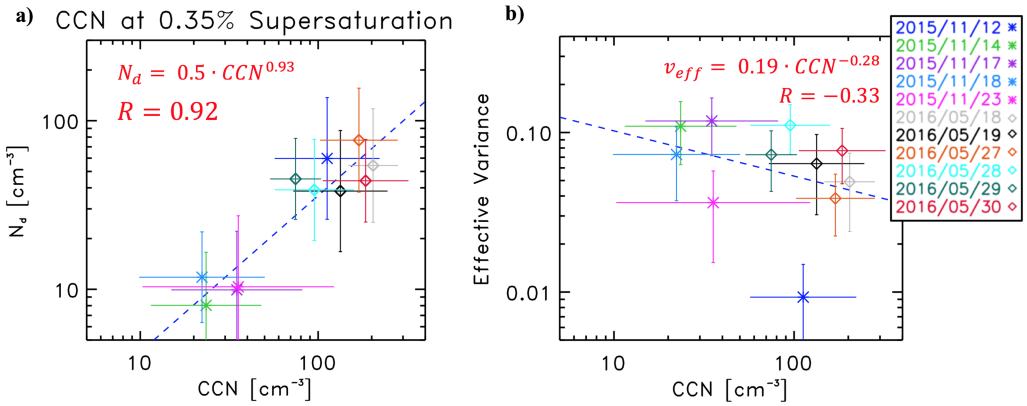

Figure 1. a) RSP N_d and in situ CCN geometric means and geometric standard deviations (bars) collected during cloud modules. b) RSP v_{eff} compared with in situ CCN. Star and diamond symbols represent data obtained during cloud modules during NAAMES-1 and NAAMES-2, respectively.

are shown for r_{eff}, v_{eff}, LWP, τ, CTH, and H. The Student's t test is used to determine the probability that the group of observations from each campaign are from the same sample population and is shown in supporting information Table S1 as the p value. All of the changes between campaigns are found to be statistically significant except meteorological changes (σ_w^2 and RH) and the change in τ.

Between campaigns, CCN concentrations increase substantially from 37 to 141 cm^{-3}. Using the AMS a large variation in aerosol mass between campaigns is found, with an average aerosol mass of 0.09 μg·m^{-3} during NAAMES-1 and 0.48 μg·m^{-3} during NAAMES-2 (supporting information Figure S13). 97% of the increase in aerosol mass is attributable to increases in sulfate and organic aerosol mass.

Notable differences in cloud properties between campaigns include a 236% increase in N_d concentrations (14 to 47 cm^{-3}), r_{eff} decreasing by 22% (13.7 to 10.7 μm), while τ increases by only 1% (14.5 to 14.7). A moderate increase in v_{eff} from NAAMES-1 to NAAMES-2 is found (0.062 to 0.066). A moderate decrease in the mean LWP from 114 g·m^{-2} during NAAMES-1 to 86 g·m^{-2} during NAAMES-2 is found, which corresponds to a decrease in average cloud physical thickness, from 1.78 km in NAAMES-1 to 1.04 km in NAAMES-2.

Considering atmospheric state parameters, the vertical wind speed's variance (σ_w^2) is found to have a small difference between campaigns, increasing from 0.144 m^2·s^{-2} during NAAMES-1 to 0.152 m^2·s^{-2} during NAAMES-2. The near cloud top RH has a 38% average during NAAMES-1 and a 33% average during NAAMES-2.

A plot detailing the covariation between remotely sensed N_d and boundary layer in situ CCN during the NAAMES-1 and NAAMES-2 campaigns is shown in Figure 1a. The plot shows daily geometric mean values of N_d and CCN for 11 science flights throughout the two campaigns. Variation in both properties is seen on daily and seasonal timescales. As expected from the Twomey effect, the Pearson correlation coefficient (R) between N_d and CCN is strong and positive ($R = 0.92$). This correlation exceeds a 99.9% confidence threshold. Spatial and temporal sampling differences between remotely sensed and in situ measurements introduces uncertainty in this comparison. Generally, Figure 1a shows that N_d and CCN observations during the NAAMES-1 campaign in the fall are lower than those observed during NAAMES-2 in the spring. Using a least squares fit, it is found that $N_d = 0.5 \cdot CCN^{0.93}$ (shown as blue dashed line in Figure 1a). The standard deviation about the regression line is 6.7. Covariation between N_d and CCN is a central concept of aerosol-cloud interactions; however, the slope of the relation is dependent on aerosol chemical composition as well as meteorological effects, which are discussed later. Measured CCN concentrations are dependent on the supersaturation that aerosols are exposed to by the CCNC and we find that correlations between N_d and CCN generally decrease when higher or lower supersaturations are assumed. For example, correlations between N_d and CCN of 0.91 and 0.49 are found at supersaturations of 0.45% and 0.25%, respectively. It also follows from the Twomey effect that r_{eff} relates inversely to CCN as observed ($R = -0.39$, supporting information Figure S14). As a proxy to cloud brightness, τ has a robust positive correlation with CCN that exceeds a 90% confidence threshold ($R = 0.54$, supporting information Figure S15).

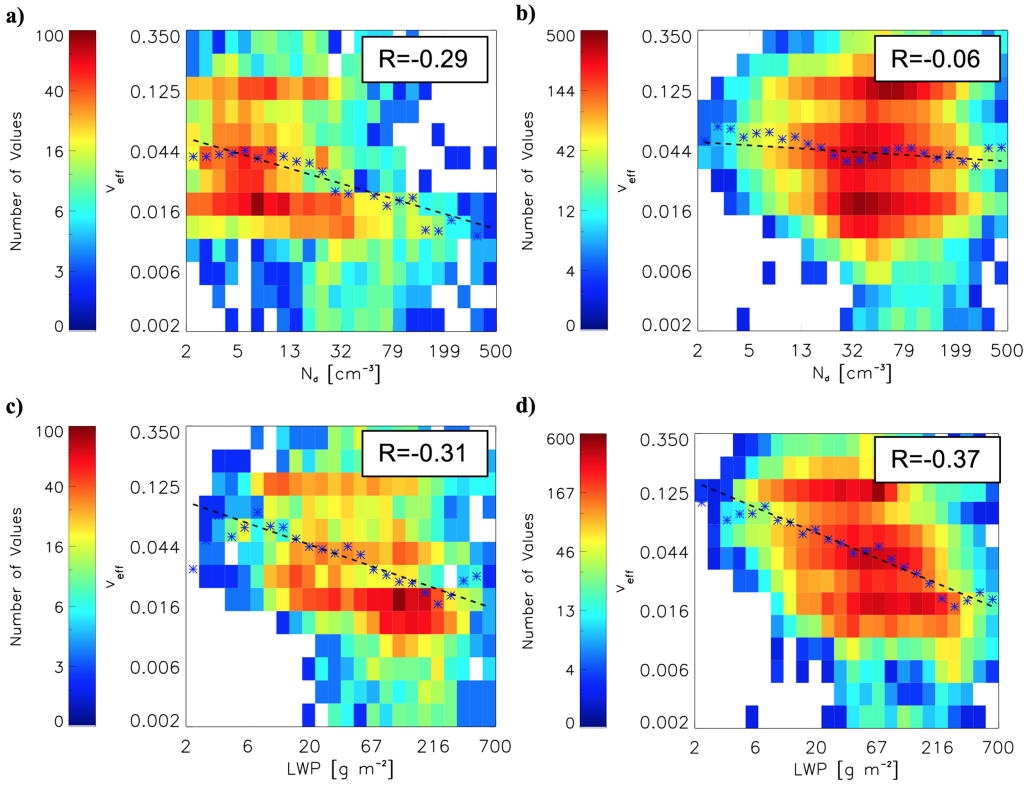

Figure 2. a) Co-variability between N_d and v_{eff} observed during NAAMES-1. Dashed line shows the least squares fit and stars indicate log mean v_{eff} value. b) Same as (a) except for NAAMES-2. c) Co-variability between LWP and v_{eff} observed during NAAMES-1. d) Same as (c) except for NAAMES-2. Color scales are different for each plot.

Secondary effects that aerosols have on cloud microphysical properties are also investigated. Figure 1b shows that throughout the 11 flights, v_{eff} is found to have a weak negative correlation with colocated CCN ($R = -0.33$) when measured at 0.35% supersaturation. Using a least squares fit, it is found that $v_{\text{eff}} = 0.19 \cdot CCN^{-0.28}$ (shown as blue dashed line in Figure 1b). The standard deviation about the regression line is 0.01. For CCN measured at supersaturations of 0.45% and 0.25% the correlation coefficients are also negative and varying from −0.33 to −0.10, respectively. Here we find that increased CCN concentrations result in smaller droplets with narrowing droplet size distributions; however, this finding is uncertain and could be supported with more comparisons.

The RSP is uniquely capable to make measurements of v_{eff} remotely and prior studies of v_{eff} are typically limited to in situ measurements made by cloud probes on aircraft while profiling clouds, we therefore place emphasis on investigating relationships involving v_{eff} in this analysis. Figure 2a shows observations of N_d and v_{eff} for NAAMES-1 including 3687 unique observations of v_{eff} and N_d from five science flights. Both of these cloud retrievals are made simultaneously by the RSP allowing each retrieval to be compared instead of colocated mean values as discussed above. The dashed line shows a least squares fit described by the relation $v_{\text{eff}} = 0.068 \cdot N_d^{-0.283}$. The correlation is found to be −0.29. The statistical significance of each correlation in Figure 2 exceeds the 95% threshold. Figure 2b shows the same results except uses 19,731 observations obtained from six science flights during NAAMES-2 yielding a correlation coefficient of −0.06 and a relation best described by $v_{\text{eff}} = 0.053 \cdot N_d^{-0.060}$. Figure 2c shows observations of LWP and v_{eff} for NAAMES-1. The dashed line shows a least squares fit described by the relation $v_{eff} = 0.12 \cdot LWP^{-0.316}$. The correlation is found to be −0.31. Figure 2d shows the same results except for NAAMES-2 and yields a correlation coefficient of −0.37 and a relation best described by $v_{\text{eff}} = 0.19 \cdot LWP^{-0.380}$. However, the reason for the strength of the correlation remains uncertain and warrants further investigation. Although a parameterization for v_{eff} based on a relationship to N_d is introduced in Morrison and Gettelman (2008), our results show a stronger relation between v_{eff} and LWP. The parametrization in Morrison and Gettelman (2008) is based on observations used

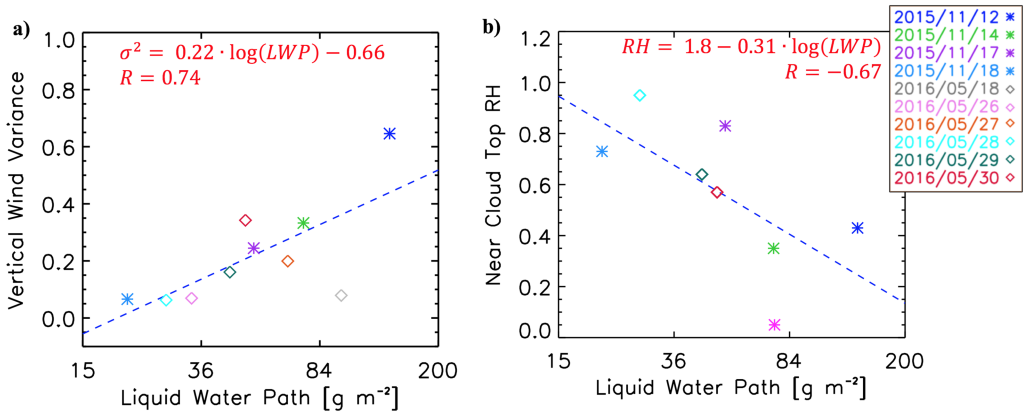

Figure 3. a) A positive correlation ($R = 0.74$) is found between LWP and vertical wind variance. b) A negative correlation ($R = -0.67$) is found between near cloud top RH and LWP. Star and diamond symbols represent data obtained during cloud modules during NAAMES-1 and NAAMES-2, respectively.

in Martin et al. (1994), who studied several cloud types in various regimes; however, this did not include the North Atlantic region.

We further investigate correlations between cloud macrophysical properties and CCN and find only a weak correlation between CCN and LWP, ($R = 0.18$, supporting information Figure S16) which indicates, as expected, that the dominant driver of LWP is unlikely CCN. Further, H and CCN are anticorrelated ($R = -0.53$), which is consistent with the cloud thinning effect resulting from increases in CCN. CTH and CCN have a similar anticorrelation ($R = -0.50$). supporting information Table S2 summarizes colocated properties, their correlation coefficients, degrees of freedom, and whether it passes the statistical significance threshold at three levels.

Meteorological conditions are investigated including σ_w^2 and RH in order to make efforts toward determining additional influences and drivers of cloud properties. Here all days in the CCN-N_d analysis are used with the exceptions of 11/23/2015 and 5/19/2016 when a low number of wind measurements were made in the boundary layer. σ_w^2 is calculated from each science flight using measurements made in the lower atmospheric layer between 0.5 and 2.0 km as a measure of atmospheric instability. Mean σ_w^2 throughout each day's cloud module varies from 0.07 $m^2 \cdot s^{-2}$ on 11/18/2015 to 0.65 $m^2 \cdot s^{-2}$ on 11/12/2015. Mean σ_w^2 from the spring campaign has more variability than the fall campaign. A weak correlation is found between σ_w^2 and N_d ($R = 0.25$, supporting information Figure S17). Throughout both campaigns, σ_w^2 is found to most strongly correlate with LWP (Figure 3a, $R = 0.74$). When averaging RH measurements made in an atmospheric layer near the cloud top region between 1.5 and 3 km, a strong anticorrelation between RH and LWP is found (Figure 3b, $R = -0.67$). Interestingly, this correlation is found to be robust with similar findings being observed in the boundary layer (supporting information Figure S19), as well as in many other atmospheric layers using a variety of vertical ranges (not shown). These findings support the notion that clouds microphysical properties respond to increases in CCN, while their macrophysical properties are less influenced changes in CCN.

Precipitation measurements were made aboard the R.V. Atlantis and therefore incorporation of precipitation analysis is limited to science flights when the cloud module and ship were colocated. Days where the aircraft and rain gauge made colocated measurements include eight of the 11 science flights from both campaigns, namely, 11/12/2015, 11/14/2015, 11/18/2015, 11/23/2015, 5/18/2016, 5/19/2016, 5/26/2016, and 5/30/2016. From this, we find that 23 November and 18 and 30 May have mean rainfall rates greater than 0.03 $mm \cdot hr^{-1}$ between 9.0 and 17.0 UTC, while little or no precipitation (<0.05 $mm \cdot hr^{-1}$) is observed on remaining days (supporting information Figures S21 and S22). Despite a relatively low number of comparison points ($n = 8$), precipitation has an anticorrelation with LWP ($R = -0.54$, supporting information Figure S23). Interestingly, precipitation is found to have a strong positive correlation with ν_{eff} ($R = 0.65$). This increase in ν_{eff} associated with precipitation could result from the RSP's ν_{eff} retrieval being affected by a bimodal cloud droplet size distribution that exists in precipitating clouds (Alexandrov, Cairns, & Mishchenko, 2012). We find a strong correlation ($R = 0.63$) when we compare the N_d and LWPs from

days when little precipitation was detected. A weak anticorrelation between precipitation and σ_w^2 ($R = -0.31$, supporting information Figure S24). Anticorrelations are also found with other cloud microphysical properties including N_d ($R = -0.14$) and r_{eff} ($R = -0.32$). A weak correlation is found between CCN and precipitation ($R = 0.26$).

4. Discussion and Conclusions

A large increase in aerosol mass and CCN concentrations is observed between the NAAMES-1 and NAAMES-2 campaigns. Sanchez et al. (2018) used a combination of radon concentrations, combustion tracers, and back trajectories to determine that few aerosols originated from continents during NAAMES-1 and NAAMES-2 with most aerosols having biogenic marine sources. These findings also agree with previous work that found that variances in marine CCN concentrations can be largely explained by DMS from a phytoplankton bloom over the North Atlantic Ocean (Cavalli et al., 2004; Yoon et al., 2007) and in other oceanic basins (Andreae et al., 1995; Charlson et al., 1987; Hegg et al., 1991).

The resulting cloud microphysical changes are found to be consistent with the Twomey effect whereby an increase in CCN concentrations result in an increase in N_d ($R = 0.92$) and, with LWP remaining constant, a decrease in r_{eff} ($R = -0.39$) and an increase in τ ($R = 0.54$; Twomey, 1977). CCN concentrations are found to have geometric mean concentrations of 37 cm^{-3} during NAAMES-1 and 141 cm^{-3} during NAAMES-2. It follows that cloud properties exhibit a similar seasonality where N_d is 236% higher, r_{eff} is 22% lower, and τ is only 1% higher during the spring (NAAMES-2) when compared with the fall (NAAMES-1).

Our analysis of NAAMES-1 and NAAMES-2 cloud properties in combination with the analysis of aerosols by Sanchez et al. (2018) suggests that cloud microphysical properties over the North Atlantic Ocean are being influenced by the phytoplankton bloom, leading to a cloud brightening effect. However, meteorological differences between the campaigns also play an important role, and therefore, the magnitude of the cloud property changes due to biogenic activity remains uncertain.

We now discuss plausible linkages from our results in context with relevant modeling and observational studies to determine which connections are supported by theory. We find that humid air surrounding the cloud top region (1.5–3.0 km) correlated negatively with LWP ($R = -0.67$), which is consistent with LES modeling studies that find dry air near cloud top enhances evaporative cooling and entrainment causing an increase in LWP, and conversely, moist overlying air is conducive to precipitation formation leading to decreased LWPs (Ackerman et al., 2004). This is also in agreement with a study of trade cumulus clouds that find that deeper cloud layers are associated with dryer boundary layers (Seifert et al., 2015). However, σ_w^2 also correlates strongly with LWP ($R = 0.74$). Therefore, a given LWP is likely a confluence of multiple parameters, such as near cloud top RH, precipitation, and boundary layer turbulence. Although cloud cover is not studied here, Seifert et al. (2015) postulate that decreased cloud top RH leads to increased evaporation of small clouds leading to a negative cloud lifetime effect.

Increases in precipitation are found to be associated with decreases in LWP ($R = -0.54$; supporting information Figure S23). This finding is supported by Ackerman et al. (2004) who found precipitation dries out cloudy air in updrafts, reducing the moisture available for evaporative cooling of downdrafts leading to a reduction of LWP. Comparing the N_d and LWPs of nonprecipitating clouds yields a strong correlation ($R = 0.63$), which is consistent with theoretical understanding (Pincus & Baker, 1994) and LES simulations that have determined the dominant response of nonprecipitating cumulus clouds to increases in N_d are increases in LWP (Bretherton et al., 2013; Seifert et al., 2015; Stevens & Seifert, 2008). We also find that precipitating clouds are strongly associated with increases in remotely sensed v_{eff} ($R = 0.65$). This increase in v_{eff} may be the result of RSP's v_{eff} retrieval being simultaneously applied to cloud and rain droplet modes, which exists in precipitating clouds, resulting in an increased average v_{eff}. However, the low number of comparison points here necessitates further investigation into this finding, possibly using a rain sensing radar alongside RSP measurements.

Our investigation found that v_{eff} has a stronger anticorrelation with LWP than with N_d. Contrary to our results, two leading global climate model parameterizations of v_{eff} either hold it as a fixed variable (Geoffroy et al., 2010) or diagnose it as an increasing function of N_d (Morrison and Gettelman, 2008).

Global climate models that parameterize v_{eff} may benefit from a focused study using RSP measurements of v_{eff} to create a realistic parameterization.

Another common measure of the width of a cloud droplet size distribution that assumes a modified gamma distribution shape is the k parameter, which is defined in terms of v_{eff} as $k = (1 - v_{\text{eff}})(1 - 2 \cdot v_{\text{eff}})$. A k value of 0.8 is a commonly used in observational retrievals and global climate models as a fixed representation of the cloud droplet size distribution width (Geoffroy et al., 2010; Grosvenor et al., 2018). A k value of 0.8 corresponds to a value of v_{eff} of 0.07. From our analysis of v_{eff}, we find that v_{eff} is lower than 0.07 68% of the time. This implies that retrievals of N_d that use a k value of 0.8 would be generally overestimating N_d in this region (Grosvenor et al., 2018). Further, these findings also suggest that models using a fixed k value of 0.8 may be underestimating the brightness of clouds in this region 68% of the time (e.g., Geoffroy et al., 2010).

With the breadth of data available from NAAMES, future work could build off current findings by implementing a CCN-N_d closure budget using the N_d, CCN, updraft velocity, and the development of a cloud droplet activation parameterization using speciated aerosols (e.g., Conant et al., 2004; Fountoukis et al., 2007). It is expected that using a regression model that accounts for aerosol chemical composition and activation saturation of CCN could partially explain unaccounted for variability in CCN measurements.

It is expected that campaign studies like this lead to better understanding of the complex processes between marine aerosols, cloud properties, and their associated feedbacks. This will enable an improved ability to accurately parameterize these small-scale properties and processes over large temporal and spatial domains. This will reduce uncertainties associated with ACIs in GCMs and thereby the uncertainty with the cloud radiative effect (Flato et al., 2013). Much needed global observations of plankton, aerosol, and cloud properties are expected to be realized with the advent of space-based polarimetry, namely, the Plankton, Aerosol, Cloud, ocean Ecosystem Satellite, which is expected to contain a multiangular polarimeter payload and be launched in 2022 (Werdell et al., 2019). This satellite will strengthen our understanding of processes linking aerosol sizes and chemical composition to clouds and their radiative properties.

Acknowledgments
The authors gratefully acknowledge insight and discussion provided by Dr. Andrew Ackerman. This work was supported in part by the National Aeronautics and Space Administration's North Atlantic Aerosol and Marine Ecosystems Study (NAAMES) and by NASA grant NNX15AD44G. Data were acquired from the NASA LaRC Airborne Science Data for Atmospheric Composition NAAMES-1 and NAAMES-2 data repositories, which are publicly available at https://www-air.larc.nasa.gov/cgi-bin/ArcView/naames.2015 and https://www-air.larc.nasa.gov/cgi-bin/ArcView/naames.2016.

References

Ackerman, A. S., Kirkpatrick, M. P., Stevens, D. E., & Toon, O. B. (2004). The impact of humidity above stratiform clouds on indirect aerosol climate forcing. *Nature*, *432*(7020), 1014–1017. https://doi.org/10.1038/nature03174

Ackerman, A. S., Toon, O. B., Taylor, J. P., Johnson, D. W., Hobbs, P. V., & Ferek, R. J. (2000). Effects of aerosols on cloud albedo: Evaluation of Twomey's parameterization of cloud susceptibility using measurements of ship tracks. *Journal of the Atmospheric Sciences*, *57*(16), 2684–2695. Chicago.

Albrecht, B. A. (1989). Aerosols, cloud microphysics, and fractional cloudiness. *Science*, *245*(4923), 1227–1230. https://doi.org/10.1126/science.245.4923.1227

Alexandrov, M. A., Cairns, B., & Mishchenko, M. I. (2012). Rainbow Fourier transform. *Journal of Quantitative Spectroscopy & Radiative Transfer*, *113*(18), 2521–2535. https://doi.org/10.1016/j.jqsrt.2012.03.025

Alexandrov, M. D., Cairns, B., Emde, C., Ackerman, A. S., & van Diedenhoven, B. (2012). Accuracy assessments of cloud droplet size retrievals from polarized reflectance measurements by the research scanning polarimeter. *Remote Sensing of Environment*, *125*, 92–111. https://doi.org/10.1016/j.rse.2012.07.012

Alexandrov, M. D., Cairns, B., Sinclair, K., Wasilewski, A. P., Ziemba, L., Crosbie, E., et al. (2018). Retrievals of cloud droplet size from the research scanning polarimeter data: Validation using in situ measurements. *Remote Sensing of Environment*, *210*, 76–95. https://doi.org/10.1016/j.rse.2018.03.005

Andreae, M. O., Elbert, W., & de Mora, S. J. (1995). Biogenic sulphur emissions and aerosols over the tropical South Atlantic. 3. Atmospheric dimethylsulfide, aerosols, and cloud condensation nuclei. *Journal of Geophysical Research*, *100*(D6), 11,335–11,356.

Bates, T. S., Kapustin, V. N., Quinn, P. K., Covert, D. S., Coffman, D. J., Mari, C., et al. (1998). Processes controlling the distribution of aerosol particles in the lower marine boundary layer during the First Aerosol Characterization Experiment (ACE 1). *Journal of Geophysical Research*, *103*(D13), 16,369–16,383. https://doi.org/10.1029/97JD03720

Behrenfeld, M. J., Moore, R. H., Hostetler, C. A., Graff, J. R., Gaube, P., Russell, L., et al. (2019). The North Atlantic Aerosol and Marine Ecosystem Study (NAAMES): Science motive and mission overview. *Frontiers in Marine Science*, *6*, 122. https://doi.org/10.3389/fmars.2019.00122

Boss, E., & Behrenfeld, M. (2010). In situ evaluation of the initiation of the North Atlantic phytoplankton bloom. *Geophysical Research Letters*, *37*, L18603. https://doi.org/10.1029/2010GL044174

Bretherton, C. S., Blossey, P. N., & Jones, C. R. (2013). Mechanisms of marine low cloud sensitivity to idealized climate perturbations: A single-LES exploration extending the CGILS cases. *Journal of Advances in Modeling Earth Systems*, *5*, 316–337. https://doi.org/10.1002/jame.20019

Bretherton, C. S., Blossey, P. N., & Uchida, J. (2007). Cloud droplet sedimentation, entrainment efficiency, and subtropical stratocumulus albedo. *Geophysical Research Letters*, *34*, L03813. https://doi.org/10.1029/2006GL027648

Cairns, B., Travis, L. D., & Russell, E. E. (1999). The Research Scanning Polarimeter: Calibration and ground-based measurements. *Proceedings of SPIE The International Society for Optical Engineering*, *3754*, 186–196.

Canagaratna, M. R., Jayne, J. T., Jimenez, J. L., Allan, J. D., Alfarra, M. R., Zhang, Q., et al. (2007). Chemical and microphysical characterization of ambient aerosols with the aerodyne aerosol mass spectrometer. *Mass Spectrometry Reviews*, *26*(2), 185–222. https://doi.org/10.1002/mas.20115

Cavalli, F., Facchini, M. C., Decesari, S., Mircea, M., Emblico, L., Fuzzi, S., et al. (2004). Advances in characterization of size-resolved organic matter in marine aerosol over the North Atlantic. *Journal of Geophysical Research*, *109*, D24215. https://doi.org/10.1029/2004JD005137

Charlson, R. J., Lovelock, J. E., Andreae, M. O., & Warren, S. G. (1987). Oceanic Phytoplankton, Atmospheric Sulphur, Cloud Albedo and Climate. *Nature*, *326*(6114), 655–661. https://doi.org/10.1038/326655a0

Christensen, M. W., & Stephens, G. L. (2011). Microphysical and macrophysical responses of marine stratocumulus polluted by underlying ships: Evidence of cloud deepening. *Journal of Geophysical Research*, *116*, D03201. https://doi.org/10.1029/2010JD014638

Conant, W. C., VanReken, T. M., Rissman, T. A., Varutbangkul, V., Jonsson, H. H., Nenes, A., & Flagan, R. C. (2004). Aerosol-cloud drop concentration closure in warm cumulus. *Journal of Geophysical Research: Atmospheres*, *109*(D13).

Fan, J., Wang, Y., Rosenfeld, D., & Liu, X. (2016). Review of aerosol-cloud interactions: Mechanisms, significance and challenges. *Journal of the Atmospheric Sciences*, *73*, 4221–4252. https://doi.org/10.1175/JAS-D-16-0037.1

Flato, G., Marotzke, J., Abiodun, B., Braconnot, P., Chou, S. C., Collins, W., et al. (2013). Evaluation of climate models. In *Climate change 2013: The physical science basis. Contribution of Working Group I to the Fifth Assessment Report of the Intergovernmental Panel on Climate Change*, (pp. 741–866). Cambridge: Cambridge University Press.

Fountoukis, C., Nenes, A., Meskhidze, N., Bahreini, R., Conant, W. C., Jonsson, H., & Flagan, R. C. (2007). Aerosol-cloud drop concentration closure for clouds sampled during the International Consortium for Atmospheric Research on Transport and Transformation 2004 campaign. *Journal of Geophysical Research: Atmospheres*, *112*(D10).

Geoffroy, O., Brenguier, J. L., & Burnet, F. (2010). Parametric representation of the cloud droplet spectra for LES warm bulk microphysical schemes. *Atmospheric Chemistry and Physics*, *10*(10), 4835–4848.

Grosvenor, D. P., Sourdeval, O., Zuidema, P., Ackerman, A., Alexandrov, M. D., Bennartz, R., et al. (2018). Remote sensing of droplet number concentration in warm clouds: A review of the current state of knowledge and perspectives. *Reviews of Geophysics*, *56*, 409–453. https://doi.org/10.1029/2017RG000593

Gultepe, I., Isaac, G. A., Leaitch, W. R., & Banic, C. M. (1996). Parameterizations of marine stratus microphysics based on in situ observations: Implications for GCMS. *Journal of Climate*, *9*, 345–357.

Hegg, D. A., Ferek, R. J., Hobbs, P. V., & Radke, L. F. (1991). Dimethyl sulfide and cloud condensation nucleus correlations in the northeast Pacific Ocean. *Journal of Geophysical Research*, *96*(D7), 13,189–13,191.

King, M. D., Radke, L. F., & Hobbs, P. V. (1993). Optical properties of marine stratocumulus clouds modified by ships. *Journal of Geophysical Research*, *98*, 2729–2739.

Liou, K. N., & Ou, S. C. (1989). The role of cloud microphysical processes in climate—An assessment from a one-dimensional perspective. *Journal of Geophysical Research*, *94*, 8599–8607.

Liu, Y., & Daum, P. H. (2002). Anthropogenic aerosols: Indirect warming effect from dispersion forcing. *Nature*, *419*(6907), 580–581. https://doi.org/10.1038/419580a

Lohmann, U., & Feichter, J. (2005). Global indirect aerosol effects: A review. *Atmospheric Chemistry and Physics*, *5*(3), 715–737.

Lu, M.-L., & Seinfeld, J. H. (2006). Effect of aerosol number concentration on cloud droplet dispersion: A large-eddy simulation study and implications for aerosol indirect forcing. *Journal of Geophysical Research*, *111*, D02207. https://doi.org/10.1029/2005JD006419

Martin, G. M., Johnson, D. W., & Spice, A. (1994). The measurement and parameterization of effective radius of droplets in warm stratocumulus clouds. *Journal of the Atmospheric Sciences*, *51*(13), 1823–1842.

Miles, N. L., Verlinde, J., & Clothiaux, E. E. (2000). Cloud droplet size distributions in low-level stratiform clouds. *Journal of the Atmospheric Sciences*, *57*(2), 295–311.

Miller, D. J., Zhang, Z., Platnick, S., Ackerman, A. S., Werner, F., Cornet, C., & Knobelspiesse, K. (2018). Comparisons of bispectral and polarimetric retrievals of marine boundary layer cloud microphysics: Case studies using a LES-satellite retrieval simulator.

Moore, R. H., & Nenes, A. (2009). Scanning flow CCN analysis—A method for fast measurements of CCN spectra. *Aerosol Science and Technology*, *43*(12), 1192–1207.

Morrison, H., & Gettelman, A. (2008). A new two-moment bulk stratiform cloud microphysics scheme in the Community Atmosphere Model, version 3 (CAM3). Part I: Description and numerical tests. *Journal of Climate*, *21*(15). 3642–3659.

Nakajima, T., & King, M. D. (1990). Determination of the optical thickness and effective particle radius of clouds from reflected solar radiation measurements. Part I: Theory. *Journal of the Atmospheric Sciences*, *47*(15), 1878–1893.

O'Dowd, C. D., Lowe, J., Smith, M. H., & Kaye, A. D. (1999). The relative importance of sea-salt and nss-sulphate aerosol to the marine CCN population: An improved multi-component aerosol-droplet parameterization. *Quarterly Journal of the Royal Meteorological Society*, *125*, 1295–1313.

Pincus, R., & Baker, M. B. (1994). Effect of precipitation on the albedo susceptibility of clouds in the marine boundary-layer. *Nature*, *372*, 250–252.

Platnick, S., Durkee, P. A., Nielsen, K., Taylor, J. P., Tsay, S.-C., King, M. D., et al. (2000). The role of back- ground cloud microphysics in the radiative formation of ship tracks. *Journal of the Atmospheric Sciences*, *57*, 2607–2624.

Platnick, S., & Twomey, S. (1994). Determining the susceptibility of cloud albedo to changes in droplet concentration with the Advanced Very High Resolution Radiometer. *Journal of Applied Meteorology*, *33*, 334–347.

Quinn, P. K., Bates, T. S., Miller, T. L., Coffman, D. J., Johnson, J. E., Harris, J. M., et al. (2000). Surface submicron aerosol chemical composition: What fraction is not sulfate? *Journal of Geophysical Research*, *105*(D5), 6785–6805. https://doi.org/10.1029/1999JD901034

Raga, G. B., & Jonas, P. R. (1993). On the link between cloud-top radiative properties and sub-cloud aerosol concentrations. *Quarterly Journal of the Royal Meteorological Society*, *119*, 1419–1425.

Roberts, G. C., & Nenes, A. (2005). A continuous-flow streamwise thermal-gradient CCN chamber for atmospheric measurements. *Aerosol Science and Technology*, *39*(3), 206–221.

Rose, D., Gunthe, S. S., Mikhailov, E., Frank, G. P., Dusek, U., Andreae, M. O., & Pöschl, U. (2008). Calibration and measurement uncertainties of a continuous-flow cloud condensation nuclei counter (DMT-CCNC): CCN activation of ammonium sulfate and sodium chloride aerosol particles in theory and experiment. *Atmospheric Chemistry and Physics*, *8*(5), 1153–1179.

Sanchez, K. J., Chen, C. L., Russell, L. M., Betha, R., Liu, J., Price, D. J., et al. (2018). Substantial seasonal contribution of observed biogenic sulfate particles to cloud condensation nuclei. *Scientific Reports*, *8*(1), 3235. https://doi.org/10.1038/s41598-018-21590-9

Seifert, A., Heus, T., Pincus, R., & Stevens, B. (2015). Large-eddy simulation of the transient and near-equilibrium behavior of precipitating shallow convection. *Journal of Advances in Modeling Earth Systems*, *7*, 1918–1937. https://doi.org/10.1002/2015MS000489

Sinclair, K., van Diedenhoven, B., Cairns, B., Yorks, J., Wasilewski, A., & McGill, M. (2017). Remote sensing of multiple cloud layer heights using multi-angular measurements. *Atmospheric Measurement Techniques*, *10*, 2361–2375. https://doi.org/10.5194/amt-10-2361-2017

Sinclair, K., van Diedenhoven, B., Cairns, B., Alexandrov, M., Moore, R., Crosbie, E., & Ziemba, L. (2019). Polarimetric retrievals of cloud droplet number concentrations. *Remote Sensing of Environment Remote Sensing of Environment*, *228*, 227–240. https://doi.org/10.1016/j.rse.2019.04.008

Stevens, B., & Seifert, A. (2008). Understanding macrophysical outcomes of microphysical choices in simulations of shallow cumulus convection. *Journal of the Meteorological Society of Japan. Series II*, *86*, 143–162.

Twohy, C. H., Petters, M. D., Snider, J. R., Stevens, B., Tahnk, W., Wetzel, M., et al. (2005). Evaluation of the aerosol indirect effect in marine stratocumulus clouds: Droplet number, size, liquid water path, and radiative impact. *Journal of Geophysical Research*, *110*, D08203. https://doi.org/10.1029/2004JD005116

Twomey, S. (1977). The influence of pollution on the shortwave albedo of clouds. *Journal of the Atmospheric Sciences*, *34*(7), 1149–1152.

Twomey, S. (1991). Aerosols, clouds and radiation. *Atmospheric Environment. Part A. General Topics*, *25*(11), 2435–2442.

Werdell, P. J., Behrenfeld, M. J., Bontempi, P. S., Boss, E., Cairns, B., Davis, G. T., et al. (2019). The Plankton, Aerosol, Cloud, ocean Ecosystem (PACE) mission: Status, science, advances. *Bulletin of the American Meteorological Society*, *100*(9), 1775–1794. https://doi.org/10.1175/BAMS-D-18-0056.1

Wood, R. (2005). Drizzle in stratiform boundary layer clouds. Part II: Microphysical aspects. *Journal of the Atmospheric Sciences*, *62*, 3034–3050.

Wood, R. (2007). Cancellation of aerosol indirect effects in marine stratocumulus through cloud thinning. *Journal of the Atmospheric Sciences*, *64*(7), 2657–2669.

Yoon, Y. J., Ceburnis, D., Cavalli, F., Jourdan, O., Putaud, J. P., Facchini, M. C., et al. (2007). Seasonal characteristics of the physico-chemical properties of North Atlantic marine atmospheric aerosols. *Journal of Geophysical Research*, *112*, D04206. https://doi.org/10.1029/2005JD007044